Proceedings of the 12th Laser Applications Forum
November 23-24, 2022
Congress Centrum Bremen

Introducing an algorithm for the automatic detection of interface positions for flange joints based on laser triangulation measurements

Ronald Pordzik*[1], Thorsten Mattulat[1]

[1] BIAS – Bremer Institut für angewandte Strahltechnik GmbH, Klagenfurter Straße 5, 28359 Bremen, Germany

Abstract

Laser brazing is a joining technique widely applied in industrial manufacturing such as automotive production. In order to establish a stable brazing process free of defects, it is necessary to support the process with a track control. Whereas conventional laser brazing processes rely on tactile track control based on the mechanical interaction between the brazing wire and the substrate surface, new approaches like the reflection-assisted laser brazing require vision-based detection of the joining interface for track control as the brazing wire is already molten when contacting the substrate surface. Especially in the case of brazing flange joints the visual detection of the interface position is challenging given the limited visual accessibility of the joint interface. Therefore, in order to reliably detect the interface position, a semi-analytic algorithm is introduced based on the signals from a laser triangulation sensor scanning the joint geometry ahead of the process zone. Hereby information about the joint geometry is used to extrapolate the surface contours of the joining partners into areas that are not visible to the sensor. The algorithm was successfully tested on 90° and 45° flange joints resulting in an uncertainty in the determination of the interface position of less than ±0.5 mm.

Keywords: laser brazing, joint interface detection, track control

1 Introduction

Automatic manufacturing such as welding and brazing is widely applied in nowadays industrial manufacturing and an integral part of industry 4.0. The automatization of processes is based on the programming of the process parameters and the teaching of the process path so that all necessary information for conducting the process is available in advance. The process path itself is determined by the shape of the workpieces. These contours in general are not ideal but rather affected by imperfections during previous machining and heat induced deformations during the automatic process. Therefore, the processing path must be controlled and adjusted during the ongoing process by feedback signals from the workpieces that can be either of visual or tactile quality. While some processes like for example conventional laser brazing processes rely on tactile track control, many other processes like laser welding or the reflection-assisted laser brazing processing approach, first introduced by Mittelstädt et al. [1], require vision-based solutions for determining and correcting the track position. Solutions for vision-based seam identification, detection and tracking were mainly researched in the application of welding processes. Previous research dealt with seam tracking of butt joints or V-grooves. Xue et al. [2] used the greyscale information of a crosshair laser to track the seam of a butt joint in a GTAW-process. Xu et al. [3] utilized the grey scale information of arc welding images by applying an edge detection algorithm on the front region between the melt pool and the seam. Kos et al. [4] calculated the position of a laser beam and the seam in 3D in real-time during laser welding with a camera and an additional illumination laser. Kiddee et al. [5] used a cross mark structured light to analyze the cross-section of a V-groove which was then matched with a template to detect the edges of the V-groove. Fan et al. [6] and Li et al. [7] were able to analyse the welding joint cross-section by a vector of the depth values, which was created by using a stripe laser. The vector of the cross-section then could be assigned to a welding joint type or profile by using the

*E-mail address of corresponding author: pordzik@bias.de

Edited by Thomas Seefeld, Tim Radel, Thorsten Mattulat
Available online at https://doi.org/10.26092/elib/1870; In: Proceedings of the 12th Laser Applications Forum, Strahltechnik, Band 76, ISBN 978-3-933762-70-2

RBF kernel function or a character string method. An algorithm which used the previous groove cross-section to locate the following one was developed and implanted by Ding et al. [8]. Thus, the seam tracking was not restricted to a certain joint type and could be applied on a free form groove.

While certain joints like for example overlap joints can be detected via rather simple algorithms, more complex joint geometries like flange joints require more sophisticated approaches to reliably detect the track position. Especially the relative position between the joint surfaces and the visual sensor is of crucial importance as it determines the number of blind spots inside the joint interface that are potentially necessary for the exact determination of the interface position. For the task of joint interface detection laser triangulation sensors have been proven as fast and reliable measuring systems [5] without the need for complex calibration while providing high data rates. During this study a semi-analytic approach for the automatized detection of joint interfaces on flange joints has been developed and tested on a set of experimental data of scanned flange joint geometries for validation.

2 Experimental setup

The joint interface profiles were measured with the laser triangulation sensor LLT 3010-50 from the manufacturer Micro-Epsilon operating at a wavelength of 658 nm with a maximum power of 10 mW. The sensor was attached to a robotic arm which was programmed to move linearly and with a constant velocity of 3000 mm/min along the joint interface. The flange joints consisted of ZnMg-coated steel sheets of the type DX56D + 100 ZnMg with an overall thickness of 0.8 mm and a coating thickness of 7 µm. The joints were set up in a clamping device with straight edges so that the joint interface positions in each cross section are expected to be arranged on a straight line. The clamping device also allows for the adjustment of the height difference between both joining partners which affects the accessibility of the joint interface by the sensor. A measuring frequency of 1000 Hz was applied resulting in a spatial resolution of 20 recorded profiles per mm in scanning direction. The exposure time used for scanning the highly reflective ZnMg-coated surfaces of the steel sheets was 200 µs. At this exposure time a sufficient illumination of the surfaces was achieved while the effects of overexposure due to the highly reflective surfaces were minimized. In the lateral direction the applied sensor provides a resolution of 2048 measuring points. At a given measuring distance of 125 mm at the top surface of the flange joint with a lateral scan field of 50 mm this results in a lateral spatial resolution of ~24 µm. With this setup two different joint geometries, a 90° flange joint with curvature radii of 2.0 mm and a 45° flange joint with radii of also 2.0 mm were scanned. In both configurations a height difference between the joining partners of 1.6 mm was applied and in all following illustrations the left metal sheet was the heightened one. Although the joint was set up in a rigid clamping device and the sensor path was programmed to follow the interface position parallelly, the height signal of the sensor is superimposed by oscillations of the robotic arm, disturbing the measuring signal. The oscillations of the robotic arm become visible in the waviness of the plane sections in the three-dimensional reconstruction of the scans as can be seen in Fig. 1 in the upper right picture.

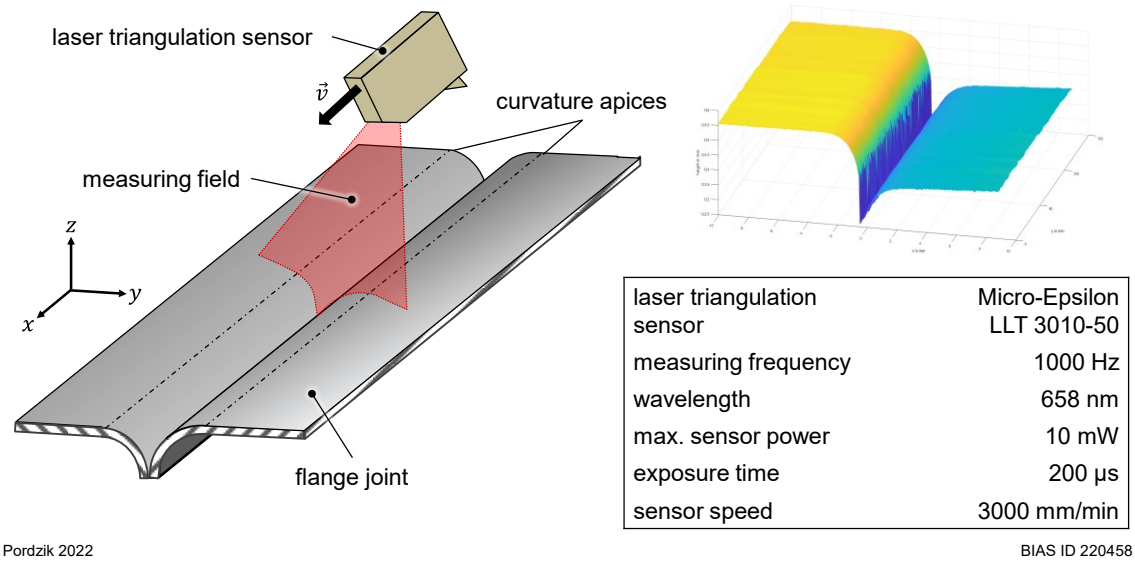

laser triangulation sensor	Micro-Epsilon LLT 3010-50
measuring frequency	1000 Hz
wavelength	658 nm
max. sensor power	10 mW
exposure time	200 µs
sensor speed	3000 mm/min

Fig. 1: Experimental setup and parameters for scanning flange joint surfaces by means of laser triangulation

3 Algorithm

The algorithm for the flange joint detection via measuring signals of a laser triangulation sensor is based on two crucial assumptions:

1. The curvatures on both sides of the flange joint can be reliably approximated by circular functions.
2. The curvature of the flange joints on both sides is preceded by an even section of arbitrary extent that serves as starting point of the calculation.

In the first step a linear regression is performed on the even sections on both sides of the flange joint starting with an initial number of points. The area of linear regression is extended iteratively on both ends of the even section until the coefficient of determination (CoD) further denoted a D surpasses a threshold defined by the CoD of the initial sample size N_{ini} following equation 1.

$$D_{\mathrm{thresh}} = 2 \cdot D_{\mathrm{ini}} \tag{1}$$

The measuring point of the laser triangulation sensor on the side of the joint interface that first surpasses the CoD threshold defines the apex of the adjacent curvature. In an analogous manner to the regression of the even section, a circular regression is performed on the curvature starting from the apex with an initial sample size of 50 measuring points.

The circular regression must fulfill the two conditions at the apex stating that itself as well as it's derivative must exhibit a continuous transition with the preceding linear section.

$$z(y = y_0) = z_0 \tag{2}$$

$$\frac{dz}{dy}\Big|_{y=y_0} = s_i = \tan(\gamma_i) \tag{3}$$

Given these two conditions the number of parameters in the regression is reduced from three to just one parameter. As the number of measuring points on the curvature is rather big compared to the number of parameters that are to be determined during the regression the resulting system of linear equations, as expressed in equation 4, is highly overdetermined and solved with regard to minimizing the CoD.

$$R \cdot [s \cdot (\boldsymbol{y} - y_0) - (\boldsymbol{z} - z_0)] = \pm\frac{\sqrt{1+s^2}}{2} \cdot [(\boldsymbol{y} - y_0)^2 + (\boldsymbol{z} - z_0)^2] \tag{4}$$

$$y_{\mathrm{c}} = y_0 \mp \frac{R}{\sqrt{1+\frac{1}{s^2}}} \qquad z_{\mathrm{c}} = z_0 \mp \frac{R}{\sqrt{1+s^2}} \tag{5}$$

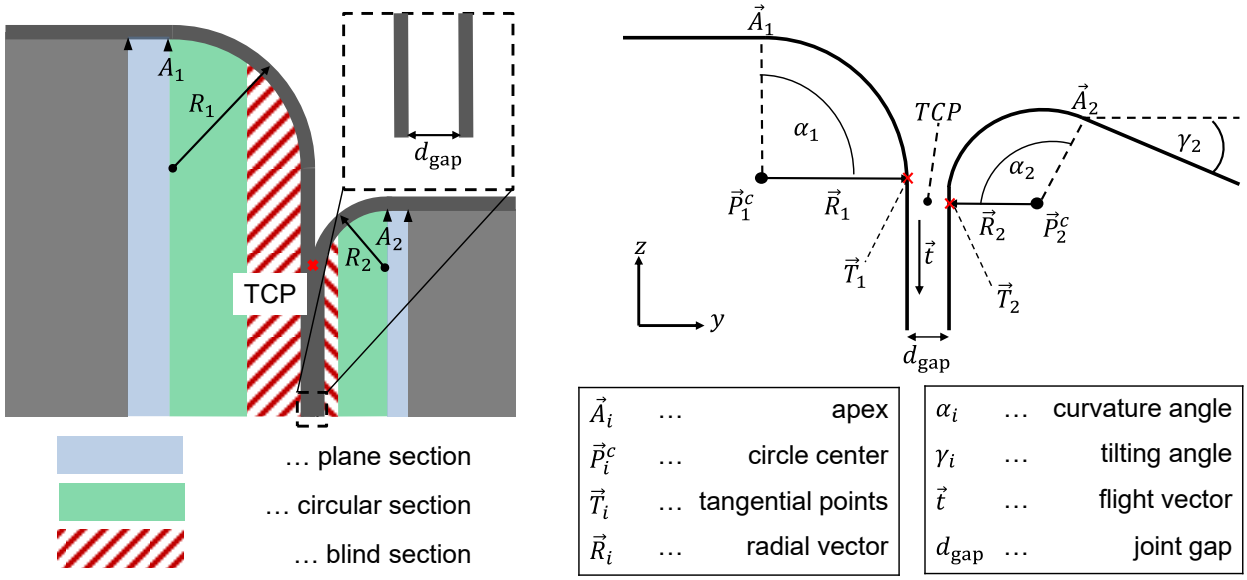

Pordzik 2022 BIAS ID 220459

Fig. 2: Schematic of the analysis sections of the joint interface (left) and the relevant geometric properties (right)

In equation 4 the parameter s denotes the slope of the respective plane section with $s_i = \tan(\gamma_i)$ and $[y_0, z_0]$ represent the 2-D coordinates of the curvature's apices. In the same manner as for the even sections the regression terminates when its CoD surpasses the threshold defined based on the initial sample of measuring points. Also, an overlap between the regions of circular regression of both sides of the joint is forbidden. By performing two regressions on each side of the flange joint the most important geometric features are determined namely the radii of the curvatures on both sides denoted by R_i as well as their respective center points $\vec{P}_i^0$ and the tilting of the whole geometry γ_i as shown in the schematic sketch from Fig. 2. The shape of the joint is required as an input parameter so that the extrapolation of the joint geometry into the concealed areas can be performed. The curvatures are extended to the required angle and prolonged tangentially from there on.

$$d_{\text{gap}} = \left| \frac{(\vec{T}_1 - \vec{T}_2) \cdot \vec{R}_1}{R_1} \right| \tag{6}$$

Now it is possible to calculate the minimum distance d_{gap} between both joining partners according to equation 6. The point where the gap at the joint interface reaches its minimum for the first time starting from the outer edges of the recorded profile is defined as the TCP, that serves as the target value for any track control that is based on this joint detection algorithm.

$$TCP = \vec{T}_i + \vec{R}_i \cdot \frac{d_{\text{gap}}}{2\, R_i} \tag{7}$$

The recorded three-dimensional profile of the joint geometry is constituted out of several two-dimensional profiles representing the cross-sections perpendicular to the moving direction of the sensor along the workpiece. The TCP can therefore be calculated for each one of these two-dimensional profiles.

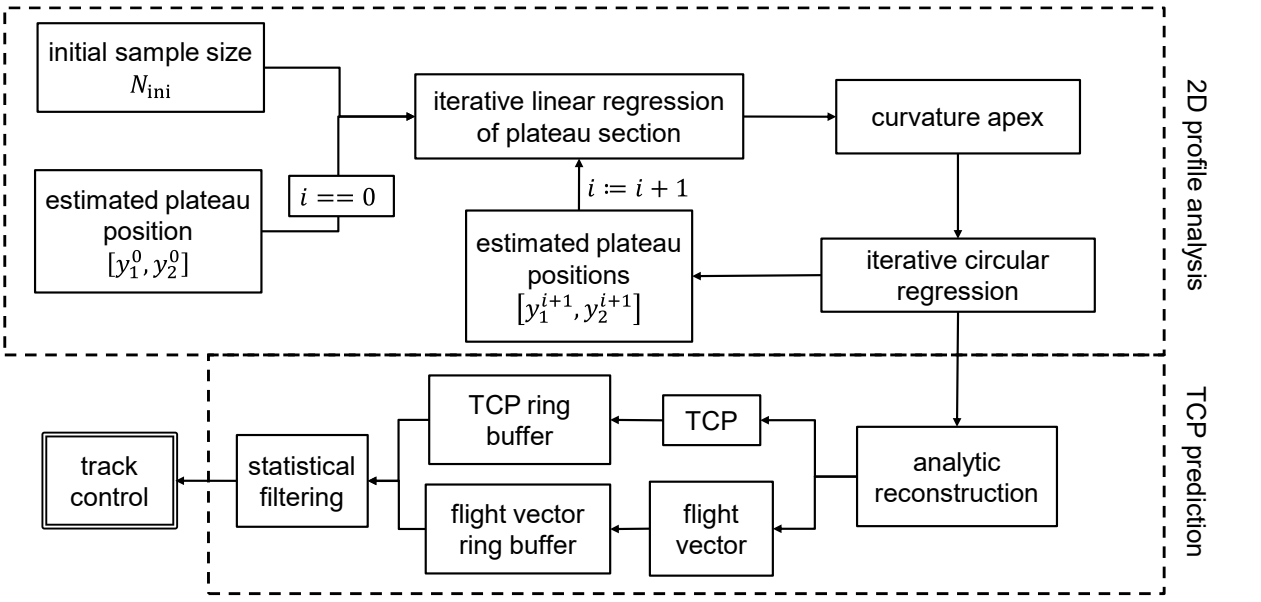

Pordzik 2022 BIAS ID 220460

Fig. 3: Block diagram of the two-phased track control algorithm consisting of joint interface detection and TCP prediction

The measurements of the flange joint surfaces are affected by the surrounding conditions as well as the condition of the reflective surface of the metal sheets and the relative position between the sensor and the surface to be measured. Therefore, not every single measured profile will provide a valid result for the TCP when it is calculated by the algorithm described above and rather must be evaluated statistically in the context with neighboring 2-D profiles. This implies that, in order to ensure the algorithm to return reliable values for the TCP, a certain number of profiles has to be recorded in advance to filter out corrupted measurements. Furthermore, the initial guess for the position of the even sections is based on the previous profiles as the shape of joint geometry along the track is expected to change in a continuous manner. The overall structure of the algorithm for joint interface detection and TCP calculation is schematically summarized in Fig. 3.

4 Results and discussion

The algorithm described in chapter 3 was applied to the scans of the two flange joint configurations described in chapter 2. The results give the y- and z-coordinates of the TCP at each profile or x-position respectively. As already mentioned, the TCPs of each cross-sectional profile are expected to be arranged on a straight line based on the construction of the clamping device. The accuracy of the algorithm is therefore characterized based on the deviations of the y- and z-coordinated of the TCP throughout the whole scanning process. The reliability of the laser triangulation sensor is limited so that not every recorded profile necessarily represents an accurate scan of the real flange joint surface. This can be for example due to overexposure of the sensor at some positions or due to signal disturbances by process emissions in case of real welding or brazing processes. To account for these influences on the measurement quality for a stable application in track control the TCP-coordinates determined for each measured profile need to be filtered. A gliding window function with a width of 20 profile scans or time steps respectively was applied to smoothen the TCP-positions. The results for the 90° flange joint are shown in Fig. 4. While, due to outliers, the accuracy based on the unfiltered TCP-positions is rather low with values of $\Delta y = \pm 1.6$ mm and $\Delta z = \pm 2$ mm, the accuracy of the smoothed TCP-positions lies in the range of $\Delta \tilde{y} = \pm 0.2$ mm and $\Delta \tilde{z} = \pm 0.4$ mm.

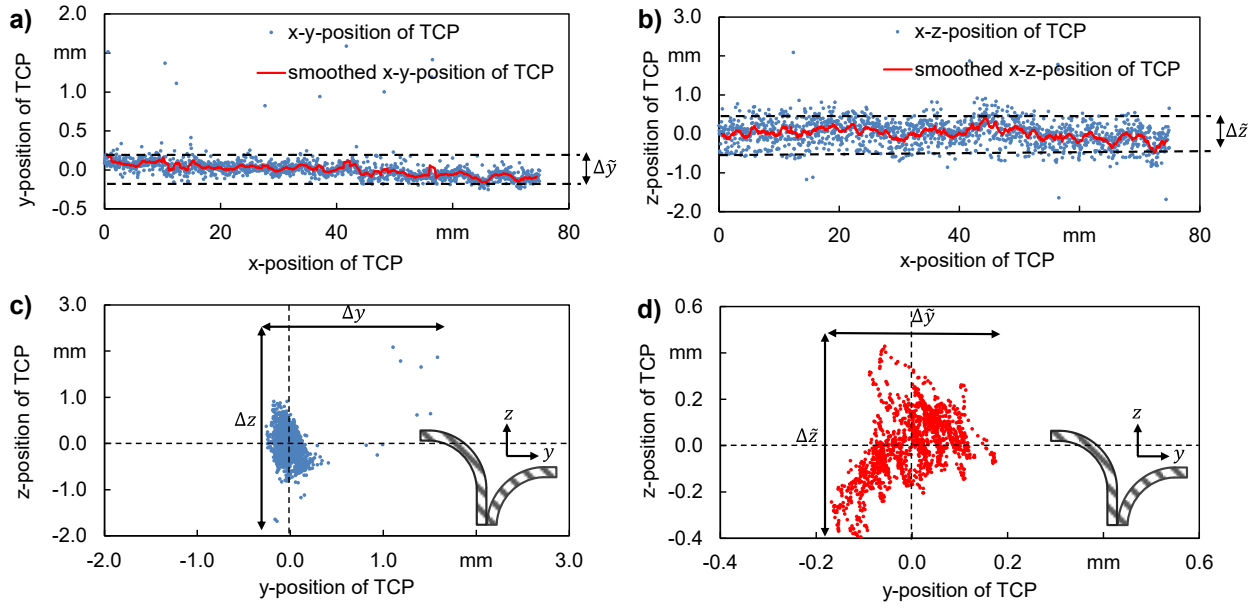

Pordzik 2022 BIAS ID 220461

Fig. 4: Results of joint interface analysis and accuracy of the interface position for the 90° flange joint: a) Scattering in the x-y-plane with and without filtering; b) Scattering in the x-z-plane with and without filtering; c) Scattering of the unfiltered interface positions in the y-z-plane; d) Scattering of the filtered interface positions in the y-z-plane

For the 45° flange joint overall higher accuracies were achieved with fewer statistical outliers diminishing the accuracy of the unfiltered TCP-positions which lie in the range of $\Delta y = \pm 0.5$ mm and $\Delta z = \pm 0.8$ mm respectively. After filtering the accuracies for the smoothed TCP-positions resulted in values of $\Delta \tilde{y} = \pm 0.2$ mm and $\Delta \tilde{z} = \pm 0.2$ mm. The corresponding results are shown in Fig. 5.

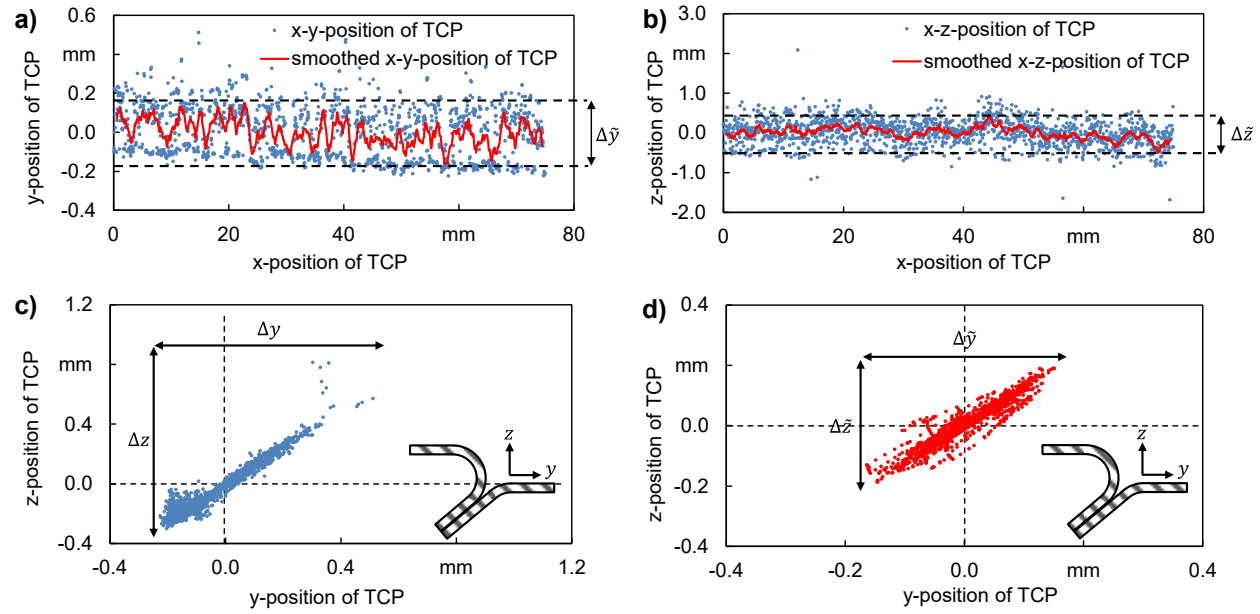

Fig. 5: Results of joint interface analysis and accuracy of the interface position for the 45° flange joint: a) Scattering in the x-y-plane with and without filtering; b) Scattering in the x-z-plane with and without filtering; c) Scattering of the unfiltered interface positions in the y-z-plane; d) Scattering of the filtered interface positions in the y-z-plane

The achieved accuracies for the smoothed TCP-position are sufficient for implementation in track control of processes like reflection-assisted laser beam brazing according to the process characterization by Henze et al. [9]. Nonetheless, the oscillations of the robotic arm and therefore the position of the laser triangulation sensor must be considered in the evaluation of the presented results. To account for these oscillations superimposed on the linear track of the sensor, the scans of the plane sections on both sides of the joint interfaces were analyzed regarding their fluctuations as depicted within Fig. 6.

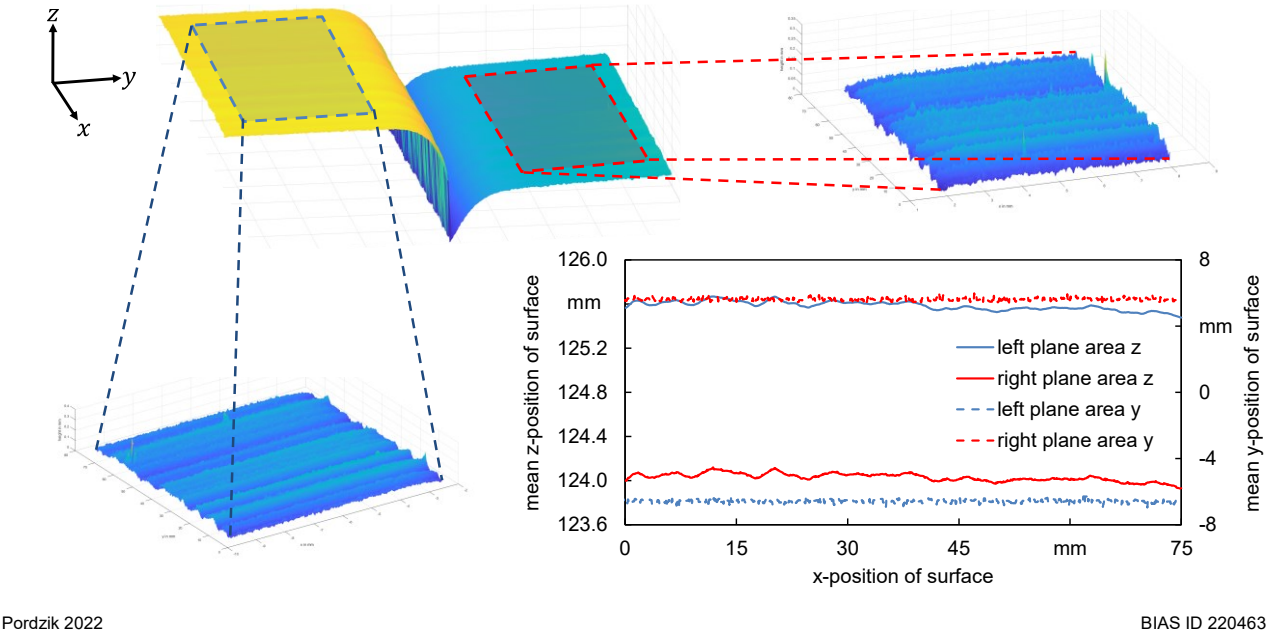

Fig. 6: Characterization of oscillations in the sensor track

The analysis of the track oscillations yields values of ±0.1 mm for the deviations from the center positions. As superpositions of track oscillations and algorithmic accuracy can lead to both amplification and attenuation of the resulting TCP-positions the resulting accuracy of the algorithms should improve by the value of the track oscillations.

5 Summary and outlook

A semi-analytic algorithm for detecting the interface positions of flange joints and adjusting the TCP has been derived and tested on experimental data. The experimental data consisted of scans of 90° and 45° flange joints recorded by a laser triangulation sensor. The joints were set up in a clamping device with straight edges, thus the joint interface positions would be arranged on a straight line which is important in order to obtain a reference for the measured interface positions. The analysis of the recorded scans resulted in fluctuations of ±2 mm for the unfiltered positions of the 90° flange joint and fluctuations of ±0.8 mm for those of the 45° flange joints. Smoothing the TCP-positions with a gliding window function and therefore reducing the effect of outliers representing corrupted measurements, much lower fluctuations of the TCP-position in the range of ±0.5 mm could be achieved for both types of joints. An analysis of the accuracy of the sensor track showed that the motion of the robotic arm is oscillating with an amplitude of ~0.1 mm around its defined center position, therefore negatively affecting the determined accuracy of the algorithm. By that the calculated accuracies of the determination of the joint interface positions must be regarded as upper limits.

Further tests of the algorithm on extended data sets are required to evaluate the potential of the algorithm for application in track control. For example, investigating the influence of lateral inclination between the sensor and the joint interface with a resulting increased blind area is necessary to assess the applicability of the method. Despite the experimental qualification of the algorithm the runtime and efficiency need to be improved to make the algorithm a suitable option for real-time track control. Yet the presented algorithm shows an accuracy in the detection of the joint interfaces sufficiently high for application in reflection-assisted laser brazing processes and therefore can be considered as a promising approach for vision-based track control for flange joint interfaces.

Acknowledgements

The ZIM-project number ZF 4587002FH9 was funded by the Federal Ministry for Economic Affairs and Energy (BMWi) via the German Federation of Industrial Research Associations (AiF) in accordance with the policy to support the Central Innovations of Medium-Sized Enterprises (ZIM) based on a decision by the German Bundestag. Furthermore, the authors gratefully acknowledge the collaboration with the members of the project affiliated committee regarding the support of knowledge, material and equipment over the course of the research. The “BIAS ID” numbers are part of the figures and allow the retraceability of the results with respect to the mandatory documentation required by the funding organization.

References

[1] C. Mittelstädt, T. Seefeld, F. Vollertsen: Laser beam brazing of hot-dip galvanized thin sheet steel in laser leading process configuration. International Congress on Applications of Lasers & Electro-Optics (2016) 1802

[2] B. Xue, B. Chang, G. Peng, Y. Gao, Z. Tian, D. Du, G. Wang: A Vision Based Detection Method for Narrow Butt Joints and a Robotic Seam Tracking. Sensors 19 (2019)

[3] Y. Xu, G. Fang, N. Lv, S. Chen, J. Zou: Computer vision technology for seam tracking in robotic GTAW and GMAW. Robotics and Computer-Integrated Manufacturing 32 (2015) 25-36

[4] M. Kos, E. Arko, H. Kosler, M. Jezeršek: Remote-laser welding system with in-line adaptive 3D seam tracking and power control. Procedia CIRP 81 (2019) 1189-1194

[5] P. Kiddee, Z. Fang, M. Tan: An automated weld seam tracking system for thick plate using cross mark structured light. The International Journal of Advanced Manufacturing Technology 87 (2016) 3589-3603

[6] J. Fan, F. Jing, Z. Fang, M. Tan: Automatic recognition system of welding seam type based on SVM method. The International Journal of Advanced Manufacturing Technology 92 (2017) 989-999

[7] X. Li, X. Li, S. Ge, M. Khyam, C. Luo: Automatic Welding Seam Tracking and Identification. IEEE Transactions on Industrial Electronics 64 (2017) 7261-7271

[8] Y. Ding, W. Huang, R. Kovacevic: An on-line shape-matching weld seam tracking system. Robotics and Computer-Integrated Manufacturing 42 (2016) 103-112

[9] I. Henze, R. Pordzik, P. Marben, T. Mattulat: Industrial applicability of reflection-assisted laser beam brazing of ZnMg-coated steel sheets. Proceedings of the 12th Laser Applications Forum (2022)